MOLECULAR AND CELLULAR BIOLOGY, Dec. 2001, p. 7944–7955 Vol. 21, No. 23
0270-7306/01/$04.00+0 DOI: 10.1128/MCB.21.23.7944–7955.2001

The Nsp1p Carboxy-Terminal Domain Is Organized into Functionally Distinct Coiled-Coil Regions Required for Assembly of Nucleoporin Subcomplexes and Nucleocytoplasmic Transport

SUSANNE M. BAILER,* CAROLIN BALDUF, AND ED HURT

Biochemie-Zentrum Heidelberg, D-69120 Heidelberg, Germany

Received 20 February 2001/Returned for modification 28 March 2001/Accepted 31 July 2001

Nucleoporin Nsp1p, which has four predicted coiled-coil regions (coils 1 to 4) in the essential carboxy-terminal domain, is unique in that it is part of two distinct nuclear pore complex (NPC) subcomplexes, Nsp1p-Nup57p-Nup49p-Nic96p and Nsp1p-Nup82p-Nup159p. As shown by in vitro reconstitution, coiled-coil region 2 (residues 673 to 738) is sufficient to form heterotrimeric core complexes and can bind either Nup57p or Nup82p. Accordingly, interaction of Nup82p with Nsp1p coil 2 is competed by excess Nup57p. Strikingly, coil 3 and 4 mutants are still assembled into the core Nsp1p-Nup57p-Nup49p complex but no longer associate with Nic96p. Consistently, the Nsp1p-Nup57p-Nup49p core complex dissociates from the nuclear pores in *nsp1* coil 3 and 4 mutant cells, and as a consequence, defects in nuclear protein import are observed. Finally, the *nsp1-L640S* temperature-sensitive mutation, which maps in coil 1, leads to a strong nuclear mRNA export defect. Thus, distinct coiled-coil regions within Nsp1p-C have separate functions that are related to the assembly of different NPC subcomplexes, nucleocytoplasmic transport, and incorporation into the nuclear pores.

The nuclear pore complex (NPC), a structural entity conserved throughout evolution, spans the nuclear membranes and thus allows exchange of molecules between the cytoplasm and nucleus (for a review, see reference 43). Its octagonal symmetry is reflected on every substructure observed in electron microscopy. Two ring-like structures consisting of eight globular units are attached to the inner and outer parts of the nuclear membrane. While the cytoplasmic ring carries short filamentous protrusions, the nuclear ring extends into a basket-like structure. Together with a central structural framework of eight spokes, both rings form a channel for the signal- and energy-dependent nucleocytoplasmic transport of molecules (15, 34).

Based on the recent analysis of isolated yeast NPCs, it is expected that only about 30 individual proteins are required to build a nuclear pore complex (35). Most of these nucleoporins (Nups) had been identified before by using either genetic or biochemical approaches (for reviews, see references 9 and 36). Affinity purification of tagged components revealed that many Nups are organized into stable subcomplexes. The Nup84p complex consists of Nup84p, Nup85p, Nup120p, and Nup145p-C, as well as Sec13p and Seh1p, and functions in mRNA export and NPC biogenesis (42). Sec13p, which is also part of the COPII coat subunit, may link endoplasmic reticulum-to-Golgi transport with nuclear envelope and NPC biogenesis (41). Nup170p was isolated in a complex with Nup157p and Nup188p (30, 33, 45).

Nsp1p is one of the most abundant Nups and is the only one known to form two distinct NPC subcomplexes (3, 18–20, 26, 35). The Nic96p complex consists of Nsp1p, Nup57p, Nup49p, and Nic96p and is located to both sides of the central gated channel and to the nuclear basket (11, 12, 18, 20, 35). The Nup82p complex is formed by Nsp1p, Nup82p, and Nup159p and is found exclusively on the cytoplasmic phase of the NPC (3, 19, 22, 26, 28, 35). Recently, the Nup116p-Gle2p subcomplex was found associated with the Nup82p complex (1, 22). Both Nsp1p complexes perform crucial functions in nucleocytoplasmic transport. Mutation or depletion of Nic96p, Nsp1p, Nup57p, or Nup49p leads to defects in protein import (4, 20, 32, 38). In addition, *nup49* mutants are impaired in mRNA export and Nup49p, Nsp1p, and Nic96p all seem to be involved in export of ribosomal large subunits (10, 24). Finally, *nup82* or *nup159* mutants show a fast onset of nuclear mRNA retention but no defect in nuclear protein import (8, 16, 19, 25).

Assembly of the heterotrimeric Nsp1p-Nup57p-Nup49p complex (later referred to as the Nup57p complex) involves the essential C-terminal domains of Nsp1p, Nup57p, and Nup49p and is a prerequisite for binding of Nic96p and its integration into the NPC (4, 37). Previous analysis of the molecular organization of the Nsp1p-Nup49p-Nup57p complex showed that Nup57p directly interacts with both Nsp1p-C and Nup49p, thus providing the organizing center of this 150-kDa complex (37). The sequence within Nsp1p-C required for formation of the Nup57p complex was located at residues 665 to 784, an area with high probability to form coiled-coil interactions. Moreover, mutation of the N-terminal coiled-coil region of Nic96p abolished its interaction with the Nsp1p-Nup57p-Nup49p complex (20, 37). Much less is known about the molecular organization of the Nup82p-Nup159p-Nsp1p complex (3, 19, 26). The C-terminal coiled-coil regions of all three components are required for stable complex formation where Nup159p-C physically interacts with Nsp1p-C and Nup82p (3, 26).

Based on its similarity in sequence and domain organization,

* Corresponding author. Present address: Universität des Saarlandes, Medizinische Biochemie und Molekularbiologie, Gebäude 44, D-66421 Homburg/Saar,Germany. Phone: 49-6841-16 265 02. Fax: 49-6841-1626027.E-mail: dr.susanne.bailer@med-rz.uni-saarland.de.

Nup p62 is considered to be the vertebrate homologue of yeast Nsp1p (6). Consistently, p62 is organized into two distinct subcomplexes. The CAN/Nup214-Nup88/Nup84-p62 complex is the counterpart of the yeast Nup82p complex (2, 14, 29). The organization of the vertebrate p62-p54-p58-p45 complex resembles that of the yeast Nsp1p-Nup57p-Nup49p complex (7, 13, 21, 23, 27, 29). Vertebrate p54 represents the Nup57p homologue and directly interacts with p62 (5, 23). Like yeast Nic96p, its higher eucaryotic homologue Nup93 associates with the p62 complex (17). Analysis of the isolated p62-p54-p58-p45 complex revealed donut-shaped particles with a diameter of 15 nm; however, its stoichiometric composition remains controversial (7, 13, 21, 27, 29).

Since Nsp1p can assemble into two distinct subcomplexes, we were interested in investigating the exact sequence requirements within Nsp1p-C for the biogenesis of the Nic96p-Nsp1p-Nup57p-Nup49p and Nup82p-Nup159p-Nsp1p complexes, as well as for nucleocytoplasmic transport. The essential Nsp1p carboxy-terminal domain (Nsp1p-C; residues 630 to 823) can be divided into four subdomains separated by short spacers (6, 37). Secondary-structure prediction of Nsp1p-C identifies three distinct regions with high probability to form α-helical coiled coils, comprising residues 680 to 730, 740 to 785, and 790 to 823, which were previously called hep-1, -2, and -3, respectively (37). In contrast, the most amino-terminal region of Nsp1p-C, including residues 630 to 665, shows a lower but still distinct likelihood to form coiled-coil interactions (37). We took a combined biochemical and mutational approach to molecularly dissect the organization of both Nsp1p subcomplexes. For this purpose, the Nsp1p-C subdomains were renamed Nsp1p coiled coils 1, 2, 3, and 4 (residues 630 to 665, 680 to 730, 740 to 785, and 790 to 823, respectively, Fig. 1A).

MATERIALS AND METHODS

Yeast strains and growth, microbiological techniques, and plasmids. The yeast strains used in this work are listed in Table 1. Cells were grown in minimal synthetic minimal complete (SDC) or yeast extract-peptone-dextrose (YPD) medium. Minimal SDC medium/plates contained all amino acids and nutrients except those used for selection. For counterselection of *URA3*-containing plasmids, 5-fluoroorotic acid (CSM medium; Bio 101, Inc., La Jolla, Calif.) was used. Genetic manipulation of yeast was performed as described in reference 40. The following yeast plasmids were used: pUN100 and pRS315, an ARS/CEN plasmid with the *LEU2* marker; pASZ11, an ARS/CEN plasmid with the *ADE2* marker; pRS315, an ARS/CEN plasmid in which the *LEU2* marker was exchanged for the *ADE2* marker; pRS314 and pRS414, ARS/CEN plasmids with the *TRP1* marker; pRS316, an ARS/CEN plasmid with the *URA3* marker; bacterial expression vectors pGEX-4T-3 (ampicillin marker) and pGEX-4T-3 (ampicillin marker replaced with the kanamycin marker), expressing a glutathione *S*-transferase (GST)-tagged protein; pET9d (kanamycin marker), expressing a GST- or His_6-tagged protein; and pET8c (ampicillin), expressing a His_6-tagged protein.

All Nsp1p, Nup159p, Nup57p, Nic96p, and Nup49p fusion proteins expressed in yeast were placed under the control of the *NOP1* promoter and tagged amino terminally with two immunoglobulin G (IgG)-binding domains derived from *S. aureus* protein A (ProtA) or green fluorescent protein (GFP). The *NSP1* fusion and truncation constructs contained the *ADHI* terminator, whereas all of the other constructs contained the authentic 3′ noncoding sequences. Expression of all constructs was verified by Western blot analysis using anti-ProtA, anti-GFP, or anti His-antibodies or by complementation. The constructs are listed in Table 2.

Mutagenesis of Nsp1p coils 3 and 4. To generate mutations within Nsp1p coils 3 and 4 leading to temperature-sensitive growth, PCR mutagenesis using *Taq* polymerase (Boehringer Mannheim) was performed under suboptimal conditions (1× BRLS buffer; 400 μM each GTP, CTP, and TTP; 200 μM ATP; 500 μM $MnCl_2$; 2.7 mM $MgCl_2$). An *NSP1-C*-specific primer initiating upstream of the *Nsi*I site and the universal primer initiating from the pUN100 backbone (1 μM each) were used for PCR. As a template, pUN100-ProtA-TEV-NSP1-C (*Nsi*I) (positions 591 to 823) was used where an *Nsi*I site was introduced at codons 723 and 724, leading to exchange of amino acids VV → AL with no effect on complementation of the *nsp1*Δ strain. The PCR products were digested with *Nsi*I/*Bam*HI and cloned into pUN100-ProtA-TEV-NSP1-C (*Nsi*I) (positions 591 to 823) that had previously been cut with *Nsi*I/*Bam*HI. The mutagenized library was first amplified in *Escherichia coli* and then transformed into the *nsp1*Δ shuffle strain. Transformants were selected on SDC-leu-ura and, after shuffling out of the wild-type plasmid on 5-fluoroorotic acid plates, tested for temperature-sensitive growth. Plasmids were reisolated from mutant cells, and the DNA was sequenced.

Purification of fusion proteins. To express His_6- or GST-tagged proteins in bacteria, cells carrying the corresponding plasmids were grown at 18°C under selective conditions to an optical density at 600 nm of 0.5 to 0.8. Expression was induced by adding 0.5 mM IPTG. After 2 h of induction, cells were harvested, washed once with water, and frozen as pellets. Cells expressing a GST fusion protein were resuspended in ice-cold HEPES buffer [20 mM HEPES (pH 7.0), 100 mM $K(CH_3COO)_2$, 2 mM $Mg(CH_3COO)_2$, 0.5 to 1% Tween 20, 2.5 mM dithiothreitol; 100 ml of induced liquid culture/5 ml of buffer] containing protease inhibitors (complete, EDTA-free protease inhibitor cocktail tablets [Boehringer Mannheim] at 1 tablet/50 ml of HEPES buffer) and lysed by sonication. Following ultracentrifugation of the lysate (1 h at 230,000 × *g*, 4°C), the supernatant was mixed with 250 μl of GSH-Sepharose beads (pre-equilibrated with 10 ml of HEPES buffer) and batch incubated for 1 h at 4°C. Following incubation, the beads were washed with 10 ml of HEPES buffer. Proteins bound to the GSH-Sepharose beads were eluted twice with 250 μl of HEPES buffer containing 10 mM GSH and stored in 10% glycerol at −20°C.

To isolate His_6-tagged proteins from bacteria, bacterial pellets corresponding to 100 ml of induced liquid culture were resuspended in 5 ml of ice-cold protein buffer PB (50 mM KP_i [pH 8.0], 150 mM NaCl, 1 mM $MgCl_2$) containing 8 M urea, and lysed by sonication. Following ultracentrifugation of the lysate (1 h at 230,000 × *g*, 4°C), the supernatant was diluted with PB to a final concentration of 4 M urea. This lysate containing His_6-tagged proteins was used for the in vitro reconstitution assay (see below). Alternatively, the lysate was applied to Ni^{2+}-NTA-agarose beads pre-equilibrated with 4 M urea/PB. Following batch incubation for 1 h at 4°C, the resin was washed three times with 1 ml of 25 mM imidazole in 4 M urea/PB. His_6-tagged proteins were eluted three times with 500 μl of 150 mM imidazole in 4 M urea/PB.

In vitro reconstitution assay. To reconstitute the Nsp1p-C subcomplexes, GST-tagged proteins previously purified via GSH-Sepharose (in the range of 1 to 1.5 μg) were mixed with cleared 4 M urea bacterial lysates expressing His_6-tagged proteins (in total, about 2 to 3 μg) or His_6-tagged proteins purified via Ni^{2+}-NTA-agarose (see above). The volume of the samples was adjusted to 500 μl with PB/4 M urea. Subsequently, the samples were renatured by extensive dialysis (molecular weight cutoff, 3,500) against PB to a final concentration of 4 mM urea. After centrifugation of the samples (15,800 × *g* at 4°C for 15 min), Tween 20 was added to a final concentration of 0.5%. The cleared lysate was mixed with 40 μl of GSH-Sepharose beads (prewashed with PB containing 0.5% Tween 20) and batch incubated for 1 h at 4°C while rotating. Unbound proteins were separated from the beads by centrifugation (3,500 × *g* at 4°C for 10 min). The GSH-Sepharose beads were washed twice with PB containing 0.5% Tween 20. To elute the bound proteins, the beads were boiled for 3 min in 30 μl of sodium dodecyl sulfate (SDS) sample buffer. Unbound proteins were analyzed by mixing the flowthrough with sodium deoxycholate and trichloroacetic acid to yield final concentrations of 0.015 and 10%, respectively. Following incubation at 4°C for 10 min, the proteins were precipitated by centrifugation (15,800 × *g* at 4°C for 15 min). The pellet was washed once with acetone at −20°C, dried, resuspended in 30 μl of SDS sample buffer, and boiled for 3 min. Equal volumes of bound and unbound proteins were analyzed by SDS-polyacrylamide gel electrophoresis (PAGE) and Coomassie staining or Western blotting.

Miscellaneous. Purification of ProtA fusion proteins from yeast, SDS-PAGE, Western blotting, expression and localization of GFP fusion proteins in yeast, and analyses of poly(A)$^+$ RNA export and nuclear protein import were done as described earlier (1). Antibodies specifically recognizing ProtA, Nsp1p-C, Nup82p, Nic96p, and Nup159p were described before (1). Anti-His monoclonal antibody MAb 13/45/31 was obtained from Dianova GmbH, Hamburg, Germany (46). In addition, the anti-His antibody from Sigma was used.

RESULTS

A novel assay for in vitro reconstitution of Nsp1p subcomplexes. To study the requirement for assembly of the different Nsp1p subcomplexes, we developed a novel in vitro reconsti-

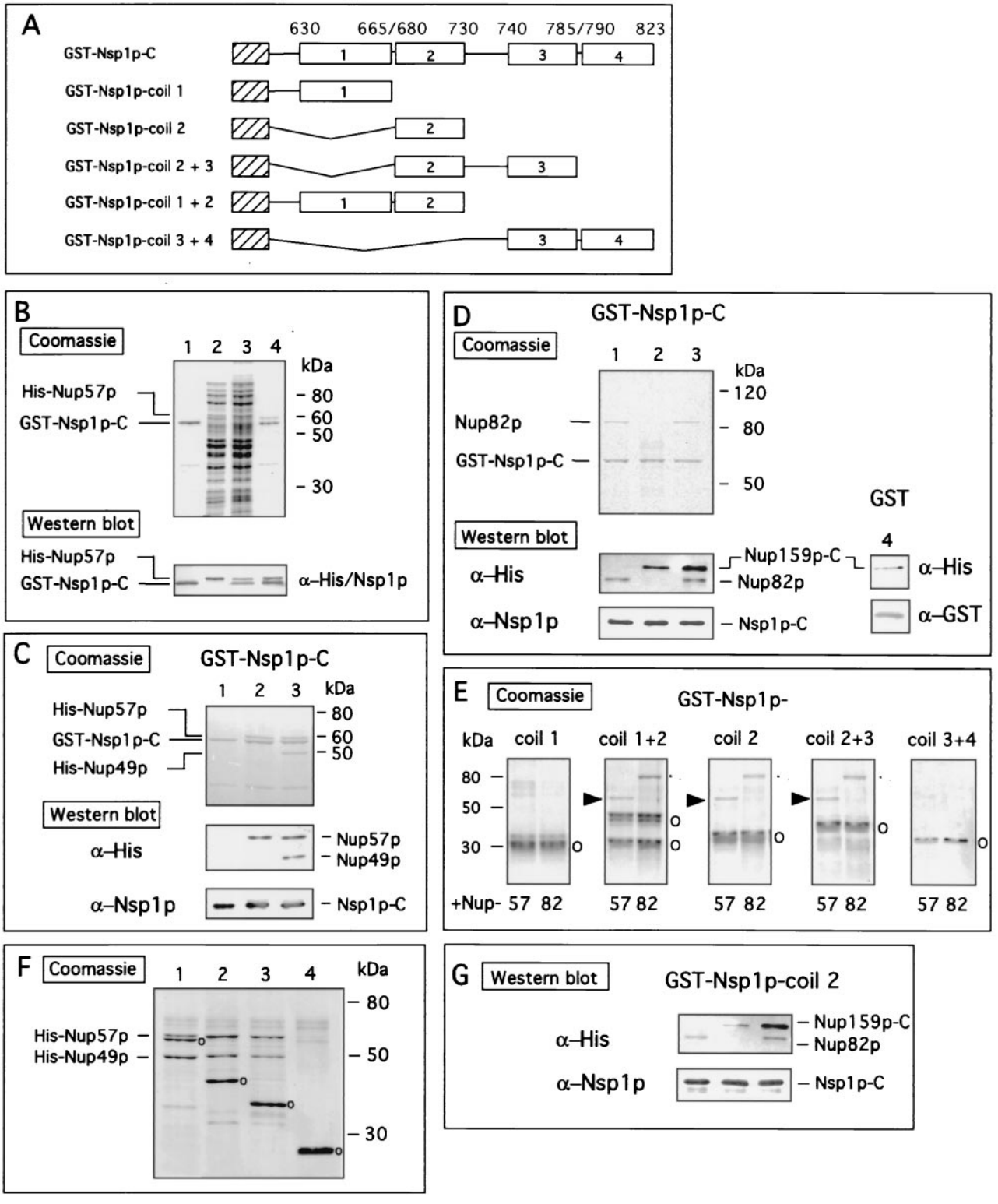

FIG. 1. In vitro reconstitution of two different heterotrimeric Nsp1p-containing complexes. (A) Schematic drawing of GST–Nsp1p-C constructs GST-Nsp1p coil 1 (positions 591 to 672), GST-Nsp1p coil 2 (673 to 738), GST-Nsp1p coils 2 and 3 (673 to 781), GST-Nsp1p coils 1 and 2 (591 to 738), and GST-Nsp1p coils 3 and 4 (728 to 823). (B) Purified GST–Nsp1p-C (lane 1) was mixed with urea-treated bacterial lysates containing His_6-Nup57p (lane 2). Proteins affinity purified via GSH-Sepharose (lane 4) were separated from unbound proteins (lane 3). (C) Purified GST–Nsp1p-C was mixed with urea-treated bacterial lysates containing His_6-Nup49p (lane 1), His_6-Nup57p (lane 2), or a mixture of both (lane 3). (D) Purified GST–Nsp1p-C (lanes 1 to 3) or GST alone (lane 4) was mixed with urea-treated bacterial lysate containing His_6-Nup82p (lane 1), His_6–Nup159p-C (lane 2 and 4), or a mixture of both (lane 3). (E) GST-tagged fragments of Nsp1p-C (as shown in panel A) were mixed with urea-treated bacterial lysate containing His_6-Nup57p or His_6-Nup82p. Open circles represent GST fusion proteins, filled triangles represent

TABLE 1. Yeast strains used in this study

Strain	Genotype	Reference
RS453	*mat***a**/α *ade2/ade2 his3/his3 leu2/leu2 trp1/trp1 ura3/ura3*	1
*nsp1*Δ shuffle	*mat*α *ade2 his3 leu2 trp1 ura3 nsp1*::*HIS3*(pRS316-URA3-NSP1)	This study
*nsp1*Δ/*nup82*Δ shuffle	*mat*α *ade2 his3 leu2 trp1 ura3 nsp1*::*HIS3 nup82*::*HIS3*(pRS316-URA3-NSP1; pRS316-URA3-NUP82)	This study
*nsp1*Δ/*nic96*Δ shuffle	*mat*α *ade2 his3 leu2 trp1 ura3 nsp1*::*HIS3 nic96*::*HIS3*(pRS316-URA3-NSP1; pRS316-URA3-NIC96)	This study
*nsp1*Δ/*nup159*Δ shuffle	*mat*α *ade2 his3 leu2 trp1 ura3 nsp1*::*HIS3 nup159*::*HIS3*(pRS316-URA3-NSP1; pLG4-URA3-NUP159 CEN)	This study
*nsp1*Δ/*nup57*Δ shuffle	*mat*α *ade2 his3 leu2 trp1 ura3 nsp1*::*HIS3 nup57*::*HIS3*(pRS316-URA3-NSP1; pRS316-URA3-NUP57)	This study

tution assay by using recombinant Nups expressed in *E. coli*. In the past, we observed that Nups containing coiled-coil domains are insoluble in *E. coli* (37). Therefore, recombinant His_6-tagged Nups had to be purified from *E. coli* lysates under denaturing conditions, renatured upon dialysis, and used for in vitro reconstitution (37) However, this procedure is time-consuming and requires large amounts of recombinant protein and only a limited number of samples can be analyzed. We found that urea-denatured GST, a widely used tag for protein purification, refolds upon dialysis and thus can be used to efficiently affinity purify in vitro-assembled NPC subcomplexes from whole-cell *E. coli* lysates. Specifically, complex formation was tested by mixing individual GST-tagged Nups with *E. coli* urea lysates containing one or several His_6-tagged Nups. After dialysis and refolding, the GST-Nup and its bound protein(s) were reisolated by glutathione (GSH) affinity chromatography (see Materials and Methods). In this way, the specificity of interaction can be tested directly by SDS-PAGE and Coomassie staining or Western blotting.

To demonstrate the applicability of this novel assay, formation of the recombinant Nsp1p-C–Nup57p complex was analyzed. GST-tagged Nsp1p-C (which corresponds to the essential C-terminal domain of Nsp1p) was expressed in *E. coli* and affinity purified. Subsequently, 1 to 1.5 μg of purified GST–Nsp1p-C (Fig. 1B, lane 1) was mixed with 8 M urea lysates of *E. coli* expressing moderate amounts of His_6-Nup57p, usually in the range of 50 ng/μl of lysate (Fig. 1B, lane 2). Following dialysis, refolded GST–Nsp1p-C, together with its associated component, was purified via GSH-Sepharose beads. Depending on the experiment, 70 to 90% of the GST-tagged protein was recovered on the GSH-Sepharose (Fig. 1B, lanes 1 and 4). As shown by Coomassie staining (top) and Western blot analysis (bottom), His_6-Nup57p was specifically coisolated with GST–Nsp1p-C (Fig. 1B, lane 4) while essentially all of the bacterial proteins remained in the unbound fraction (Fig. 1B, lane 3). To reinvestigate the association of the trimeric Nsp1p-C–Nup57p–Nup49p complex, GST–Nsp1p-C was mixed with 8 M urea lysates of *E. coli* expressing either His_6-Nup57p, His_6-Nup49p, or lysates of both. As shown by Coomassie staining (top) and Western blot analysis (bottom), His_6-Nup57p was specifically coisolated with GST–Nsp1p-C independently of Nup49p (Fig. 1C, lane 2). In contrast, His_6-Nup49p was bound to GST–Nsp1p-C only in the presence of Nup57p (Fig. 1C, lanes 1 and 3). In further controls, we could show that neither His_6-Nup49p nor His_6-Nup57p was bound to the GST tag alone or to GSH-Sepharose beads (data not shown; see also Fig. 1F). Thus, with our novel in vitro reconstitution assay, previous data on the assembly of the Nsp1p-C–Nup57p–Nup49p complex could be corroborated. In addition, the fact that His_6-Nup49p and His_6-Nup57p were specifically fished by GST–Nsp1p-C from an *E. coli* whole-cell lysate demonstrates the specificity of the interaction between these proteins.

To reconstitute the Nup82p–Nup159p-C–Nsp1p-C complex in vitro, the pulldown assay described above was applied. Purified GST–Nsp1p-C was mixed with 8 M urea lysates of bacterial cells expressing His_6-Nup82p, His_6–Nup159p-C, or lysates of both (Fig. 1D). SDS-PAGE, followed by Coomassie staining (top) and Western blot analysis (bottom), revealed that both Nup82p and Nup159p-C were able to bind to Nsp1p-C independently of each other (Fig. 1D, lanes 1 and 2). Nup82p specifically binds to certain subdomains of Nsp1p-C but not to GST alone (Fig. 1E and data not shown), whereas Nup159p-C also interacts, to a certain extent, unspecifically with the GST tag (Fig. 1D, lane 4). However, the amount of Nup159p-C that binds to GST–Nsp1p-C is significantly enhanced when Nup82p is present during in vitro reconstitution, indicating that Nup82p is crucial for efficient Nup82p–Nup159p–Nsp1p-C complex formation. Thus, our novel assay allowed the in vitro reconstitution of both Nsp1p-C subcomplexes and showed for the first time that Nup82p, like Nup57p, physically interacts with Nsp1p-C.

A minimal region of 66 residues within Nsp1p-C is sufficient for formation of both heterotrimeric complexes. Since Nup57p and Nup82p directly interact with Nsp1p-C, it was of interest to investigate whether these proteins bind to the same region or different regions within Nsp1p-C. Previously, the region required for interaction with Nup57p-Nup49p was mapped to residues 665 to 784 (which corresponds to Nsp1p coils 2 and 3 in Fig. 1A; see also reference 37). To identify the minimal interaction domain for Nup57p and Nup82p within Nsp1p-C, GST-tagged fragments of Nsp1p-C were affinity purified from *E. coli* and subsequently mixed with bacterial lysates containing

Nup57p, and open triangles represent Nup82p. (F) GST–Nsp1p-C (lane 1), GST-Nsp1p coils 2 and 3 (lane 2), GST-Nsp1p coil 2 (lane 3), or GST alone (lane 4) was mixed with urea-treated bacterial lysate containing His_6-Nup49p and His_6-Nup57p. (G) GST-Nsp1p coil 2 (lanes 1 to 3) was mixed with urea-treated bacterial lysate containing His_6-Nup82p (lane 1), His_6–Nup159p-C (lane 2), or a mixture of both (lane 3). For panels B to G, dialysis of the protein mixture was followed by affinity purification of the reconstituted GST-Nsp1p subcomplexes or of GST on glutathione-Sepharose. Proteins eluted from the column were analyzed by SDS-PAGE and Coomassie staining or Western blotting with anti-His, anti-Nsp1p, or anti-GST antibodies.

TABLE 2. Plasmids used in this study

Plasmid	Comment(s)	Reference
pUN100-LEU2-ProtA-TEV-NSP1-(591–823) (NsiI)	Construct contains an *Nsi*I site changing amino acids 724 and 725 (VV) into (AL); called *NSP1-C* or Nsp1p-C	This study
pRS315-ADE2-GFP-NSP1-(591–823)	Like construct 1; ProtA replaced by GFP; called GFP-Nsp1p-C in Fig. 5	This study
pUN100-LEU2-ProtA-nsp1 ts18	See Materials and Methods; called *nsp1 ts18* in Fig. 3, 4, and 5	This study
pRS315-ADE2-GFP-nsp1 ts18	Like construct 3; ProtA replaced by GFP; called GFP-*nsp1 ts18* in Fig. 5	This study
pUN100-LEU2-ProtA-TEV-nsp1-(591–775)	Called *nsp1 tsΔ4* in Fig. 3	This study
pSB32-LEU2-pADH-NSP1-L640S	Called *nsp1-L640S* in Fig. 3 and 4	44
pUN100-LEU2-ProtA-TEV-NSP1-(630–823) (ΔN)	Called *nsp1-(630–823)* in Fig. 3	This study
pUN100-LEU2-ProtA-TEV-NSP1-(638–823)	Called *nsp1-(638–823)* in Fig. 3	This study
pUN100-LEU2-ProtA-TEV-NSP1-(642–823)	Called *nsp1-(642–823)* in Fig. 3	This study
pSB32-LEU2-pADH-nsp1-ala6	Called *nsp1-ala6* in Fig. 3 and 4	3
YCplac33-URA3-NUP159 (pLG4)		8
pRS316-URA3-NUP82		19
pCH1122-URA3-ADE3-NIC96		20
pRS316-URA3-NUP57		20
pRS414-TRP1-GFP-NUP159-(2–1460)	Called GFP-Nup159p in Fig. 4 and 5	1
pRS314-TRP1-GFP-NIC96-(2–838)	Called GFP-Nic96p in Fig. 5	1
pRS314-TRP1-GFP-NUP57-(2–541)	Called GFP-Nup57p in Fig. 5	This study
pRS314-TRP1-GFP-NUP82-(2–713)	Called GFP-Nup82p in Fig. 4 and 5	1
pRS315-ADE2-GFP-NPL3 (283–397)	Called GFP-Npl3p in Fig. 4	39
pGEX-4T-3 (Kan)-GST-NSP1-C (591–823)	Ampicillin resistance was released from pGEX-4T-3 and replaced by kanamycin resistance; called GST-Nsp1p-C in Fig. 1 and 2	This study
pGEX-4T-3 (Amp)-GST-NSP1-(591–672)	Called GST-Nsp1p-coil 1 in Fig. 1	This study
pGEX-4T-3 (Kan)-GST-NSP1-(673–781)	Called GST-Nsp1p-coil 2 + 3 in Fig. 1	This study
pGEX-4T-3 (Kan)-GST-NSP1-(673–738)	Called GST-Nsp1p-coil 2 in Fig. 1	This study
pGEX-4T-3 (Amp)-GST-NSP1-(591–738)	Called GST-Nsp1p-coil 1 + 2 in Fig. 1	This study
pGEX-4T-3 (Amp)-GST-NSP1-(728–823)	Called GST-Nsp1p-coil 3 + 4 in Fig. 1	This study
pET9d (Kan)-GST-NUP57-(2–541)	Called GST-Nup57p in Fig. 2	This study
pET9d (Kan)-His6-NSP1-(591–823)	Called His6-Nsp1p-C in Fig. 2	This study
pET9d (Kan)-His6-NUP159-(892–1460)	Called His6-Nup159p-C in Fig. 1	This study
pET8c (Amp)-His6-NUP49-(2–472)	Called His6-Nup49p in Fig. 1	37
pET8c (Amp)-His6-NUP57-(2–541)	Called His6-Nup57p in Fig. 1 and 2	37
pET8c (Amp)-His6-NUP82-(2–713)	Called His6-Nup82p in Fig. 1 and 2	37

His_6-Nup82p or His_6-Nup57p. Affinity purification of GST-Nsp1p coil 1 (residues 591 to 672), GST-Nsp1p coil 2 (residues 673 to 738), GST-Nsp1p coils 1 and 2 (residues 591 to 738), GST-Nsp1p coils 2 and 3 (residues 673 to 780), or GST-Nsp1p coils 3 and 4 (residues 728 to 823) showed that only those fragments containing Nsp1p coil 2 were able to form heterodimeric complexes with His_6-Nup82p or His_6-Nup57p (Fig. 1E). In contrast, neither GST-Nsp1p coil 1 nor GST-Nsp1p coils 3 and 4 interacted with either of these proteins. Thus, Nsp1p coil 2 (residues 673 to 738) represents the critical region for interaction with Nup57p and Nup82p.

Since Nup82p and Nup57p mediate the interaction of Nsp1p-C with Nup159p-C and Nup49p, respectively, it was expected that Nsp1p coil 2 is also sufficient for formation of the heterotrimeric subcomplexes. Therefore, GST-Nsp1p coil 2 was combined with urea lysates containing His_6-Nup49p and/or His_6-Nup57p (Fig. 1F). Likewise, GST-Nsp1p coil 2 was mixed with lysates containing His_6-Nup82p and/or His_6–Nup159p-C (Fig. 1G). Apparently, GST-Nsp1p coil 2 is able to form heterotrimeric complexes either with Nup57p and Nup49p or with Nup82p and Nup159p-C (Fig. 1F and G). As shown for GST–Nsp1p-C, Nup82p and Nup159p-C both interact with GST-Nsp1p coil 2; however, binding of Nup159p-C is much more efficient in the presence of Nup82p (Fig. 1D and G, lanes 1 to 3). Thus, Nsp1p coil 2 (residues 673 to 738) represents the minimal region required for the formation of both heterotrimeric Nsp1p subcomplexes.

Nup82p and Nup57p compete for binding to Nsp1p-C. The finding that a short region of 66 residues within Nsp1p-C (residues 673 to 738) is sufficient for the formation of both Nsp1p-C subcomplexes implies that binding of Nup57p to this Nsp1p-C region could interfere with the binding of Nup82p. To test for this, the in vitro reconstitution assay was performed by mixing GST-tagged Nup57p with *E. coli* lysates containing His_6–Nsp1p-C and/or His_6-Nup82p (Fig. 2A). Affinity purification of GST-Nup57p showed that only His_6–Nsp1p-C was coisolated while His_6-Nup82 remained in the unbound fraction (Fig. 2B, lane 1). When GST-Nup57p was incubated with lysate containing His_6-Nup82p in the absence of Nsp1p-C, again no interaction was observed (Fig. 2B, lane 2). This is further evidence that Nup57p and Nup82p do not directly interact. However, when incubated with GST–Nsp1p-C, His_6-Nup82p was strongly recovered in the bound fraction (Fig. 2B, lane 3). This indicates that in the absence of Nup57p, His_6-Nup82p present in the *E. coli* lysate is able to bind to Nsp1p-C.

To show directly that Nup57p and Nup82p compete for the same binding site on Nsp1p coil 2 (residues 673 to 738), competition experiments were performed. GST–Nsp1p-C was incubated with *E. coli* lysates containing His_6-Nup82p in the absence or presence of increasing amounts (in the range of 0.06 to 9.6 μg) of purified His_6-Nup57p (Fig. 2C). As shown by SDS-PAGE analysis and Coomassie staining or by Western blotting, purification of GST–Nsp1p-C following dialysis revealed binding of Nup82p in the absence of His_6-Nup57p (Fig.

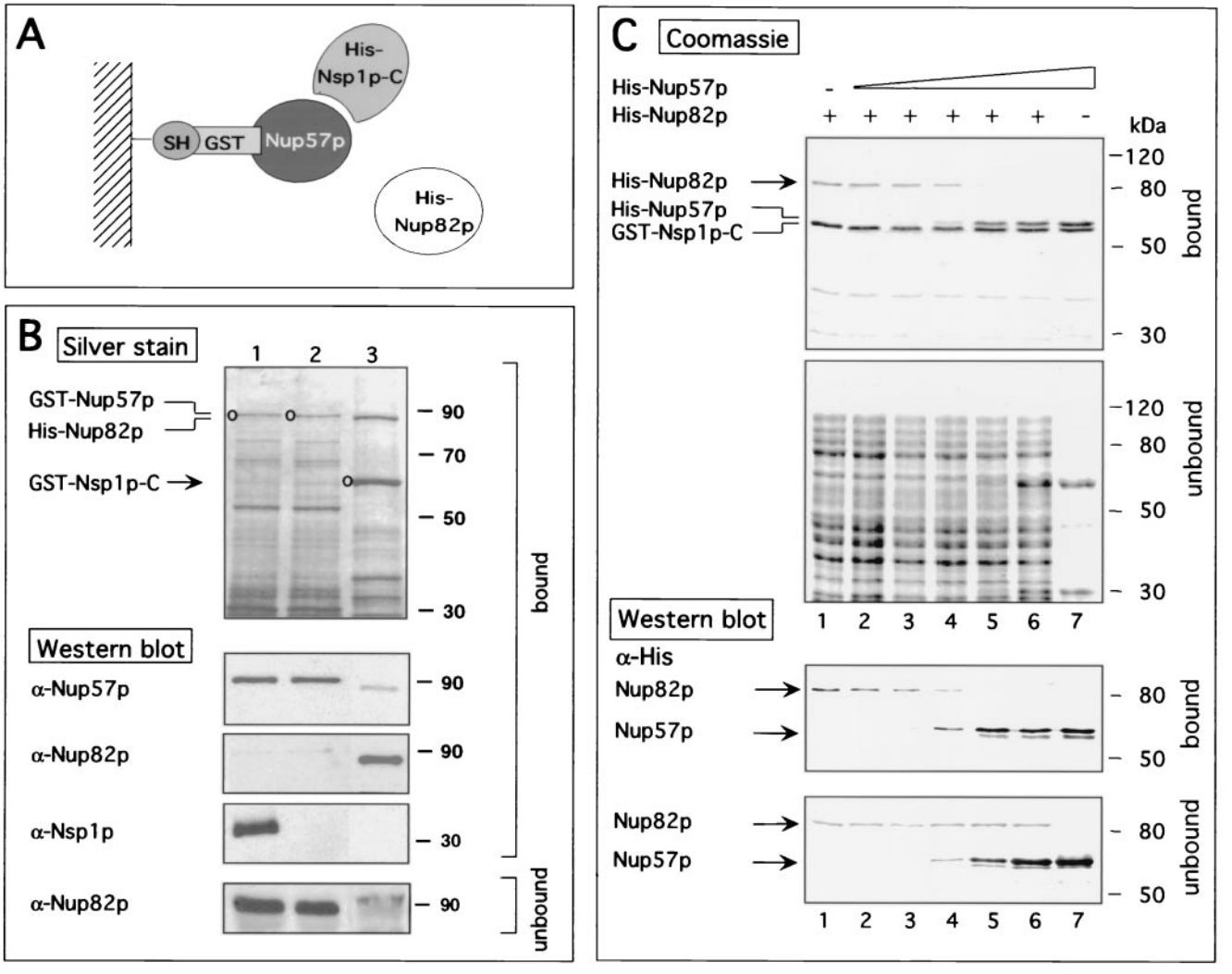

FIG. 2. Nup82p and Nup57p compete for binding to Nsp1p-C. (A) Schematic drawing of the competition assay. (B) GST-Nup57p (lanes 1 and 2, indicated by open circles) or GST–Nsp1p-C (lane 3, indicated by an open circle) was mixed with urea-treated bacterial lysate containing His_6-Nup82p and His_6–Nsp1p-C (lane 1) or only His_6-Nup82p (lane 2 and 3). In vitro reconstitution was performed as described in the legend to Fig. 1. Proteins eluted from the glutathione-Sepharose or unbound proteins were analyzed by SDS-PAGE, followed by silver staining or Western blotting with anti-Nup57p, anti-Nup82p, or anti-Nsp1p antibodies. GST-Nsp1p, used in lane 3, is not shown in the Western blot. The band seen in the anti-Nup57p Western blot (lane 3) results from the first incubation of this membrane with anti-Nup82p antibodies and thus represents His_6-Nup82p. (C) GST–Nsp1p-C was mixed with bacterial lysates containing His_6-Nup82p (lane 1), both His_6-Nup82p lysate and increasing amounts of purified His_6-Nup57p (lanes 2 to 6), or His_6-Nup57p alone (lane 7). In vitro reconstitution was performed as described in the legend to Fig. 1, and proteins eluted from glutathione-Sepharose were analyzed by SDS-PAGE and Coomassie staining or Western blotting with anti-His antibodies.

2C, lane 1). However, binding of Nup82p was progressively inhibited by addition of increasing amounts of His_6-Nup57p (Fig. 2C, lanes 2 to 6). Thus, Nup57p efficiently competes with Nup82p for assembly with Nsp1p-C. This all shows that coiled-coil region 2 of Nsp1p-C (residues 673 to 738) represents an area required for the formation of two distinct and mutually exclusive Nsp1p subcomplexes.

Mutational analysis of coiled-coil regions 1, 3, and 4 of Nsp1p-C. Most of the *nsp1* temperature-sensitive (ts) mutants obtained map within Nsp1p coil 2, which organizes two different heterotrimeric complexes (e.g., *nsp1-ala6*, *nsp1-E706P/L707S* [ts10A], and *nsp1-E706P* [tsS5]; see also references 18, 31, and 32). Consistently, the *nsp1-ala6* mutation affects the integrity of both subcomplexes (3). However, the role of the other coiled-coil regions of Nsp1p-C remained unknown. To analyze the functional importance of Nsp1p coil 1 (630 to 665), this region was progressively shortened from its N terminus (Fig. 3). Deletion of adjacent residues 591 to 630, for which no coiled-coil formation is predicted, did not impair the function of Nsp1p in vivo (Fig. 3A and B, lane 2). However, deletion of only 8 to 12 residues from Nsp1p coil 1 [e.g., Nsp1p (638–823)] caused slow growth at 23 and 30°C and a ts phenotype at 37°C. Further shortening of coiled-coil region 1 led to lethality [e.g., Nsp1p (646–823) and Nsp1p (664–823); data not shown]. Point mutations mapping within coiled-coil region 1 (e.g., *nsp1-L640S* and *nsp1-W644C*) also led to a ts phenotype (44; U.

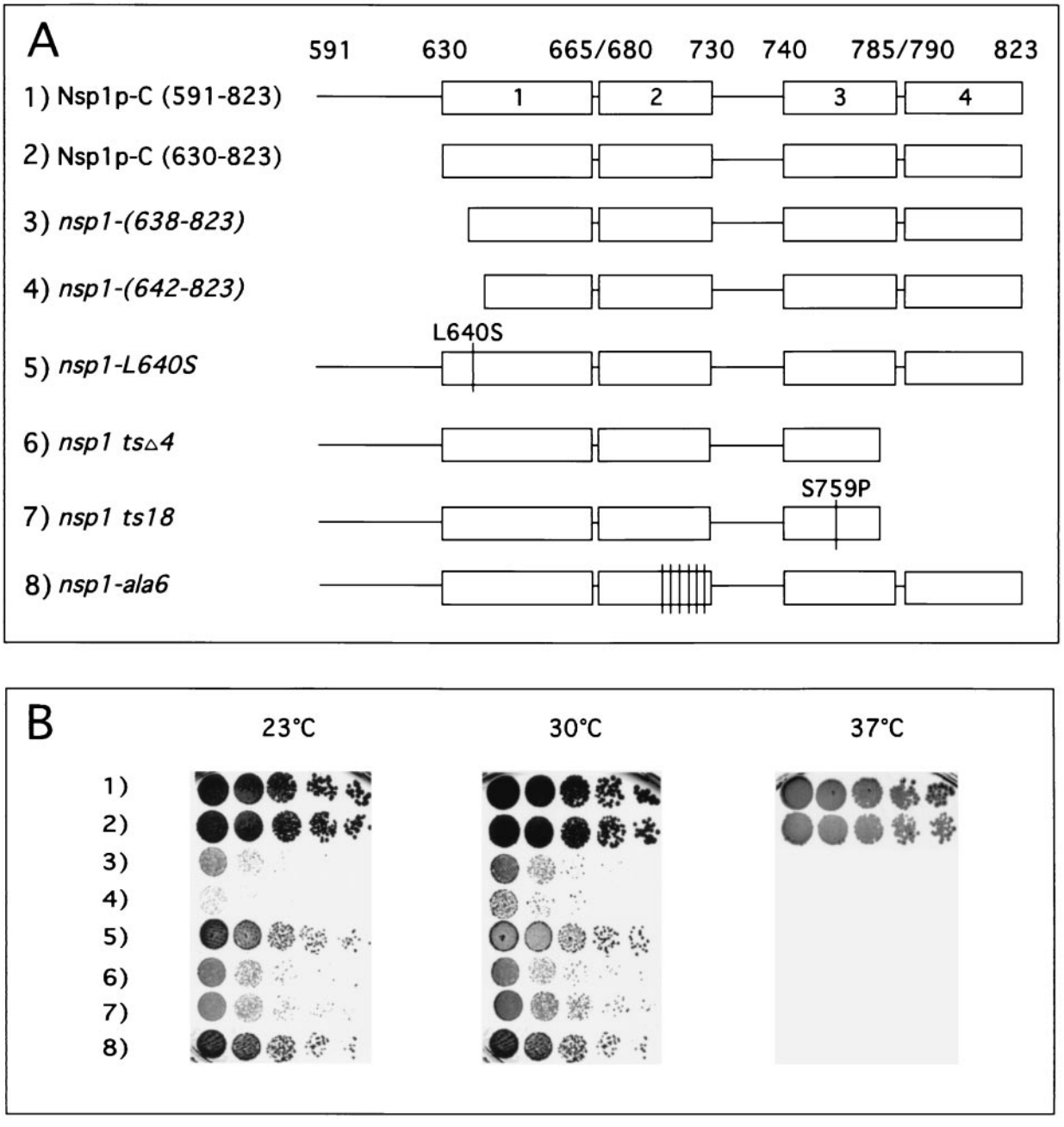

FIG. 3. Mutational analysis of the various coiled-coil regions within Nsp1p-C. (A) Schematic drawings of Nsp1p-C (591–823) (map 1), Nsp1p-C (630–823) (map 2), *nsp1-(638–823)* (map 3), *nsp1-(642–823)* (map 4), *nsp1-L640S* (map 5), *nsp1 tsΔ4* (map 6), *nsp1 ts18* (map 7), and *nsp1-ala6* (map 8). (B) Growth properties of Nsp1p-C and *nsp1* ts cells as indicated in panel A. In each case, the *nsp1*Δ strain was complemented by a plasmid expressing the corresponding mutant (see Table 2). Precultures were diluted in 10^{-1} steps, and equivalent amounts of cells were dropped on YPD plates and incubated at 23, 30, or 37°C for 3 to 4 days.

Nehrbass and E. C. Hurt, unpublished data). Thus, although not required for complex formation, Nsp1p coil 1 is an essential region within Nsp1p-C.

To analyze the function of Nsp1p coils 3 and 4, random ts mutants were generated in these domains, and two of them, *nsp1-S759P*/*Δ776–823* (*nsp1 ts18*) and *nsp1-Δ776–823* (*nsp1 tsΔ4*), were analyzed further (Fig. 3). Both mutants carry a complete deletion of coiled-coil region 4 that causes impaired growth at 23 and 30°C and growth arrest at 37°C. Thus, in contrast to Nsp1p coil 1, Nsp1p coil 4 is dispensable for cell viability but required for optimal growth. Altogether, the region of Nsp1p-C required for viability at 37°C correlates well with predicted coiled-coil regions 1, 2, 3, and 4, comprising residues 630 to 823.

The different Nsp1p-C subdomains are involved in nucleocytoplasmic transport. The findings that Nsp1p coils 1, 3, and

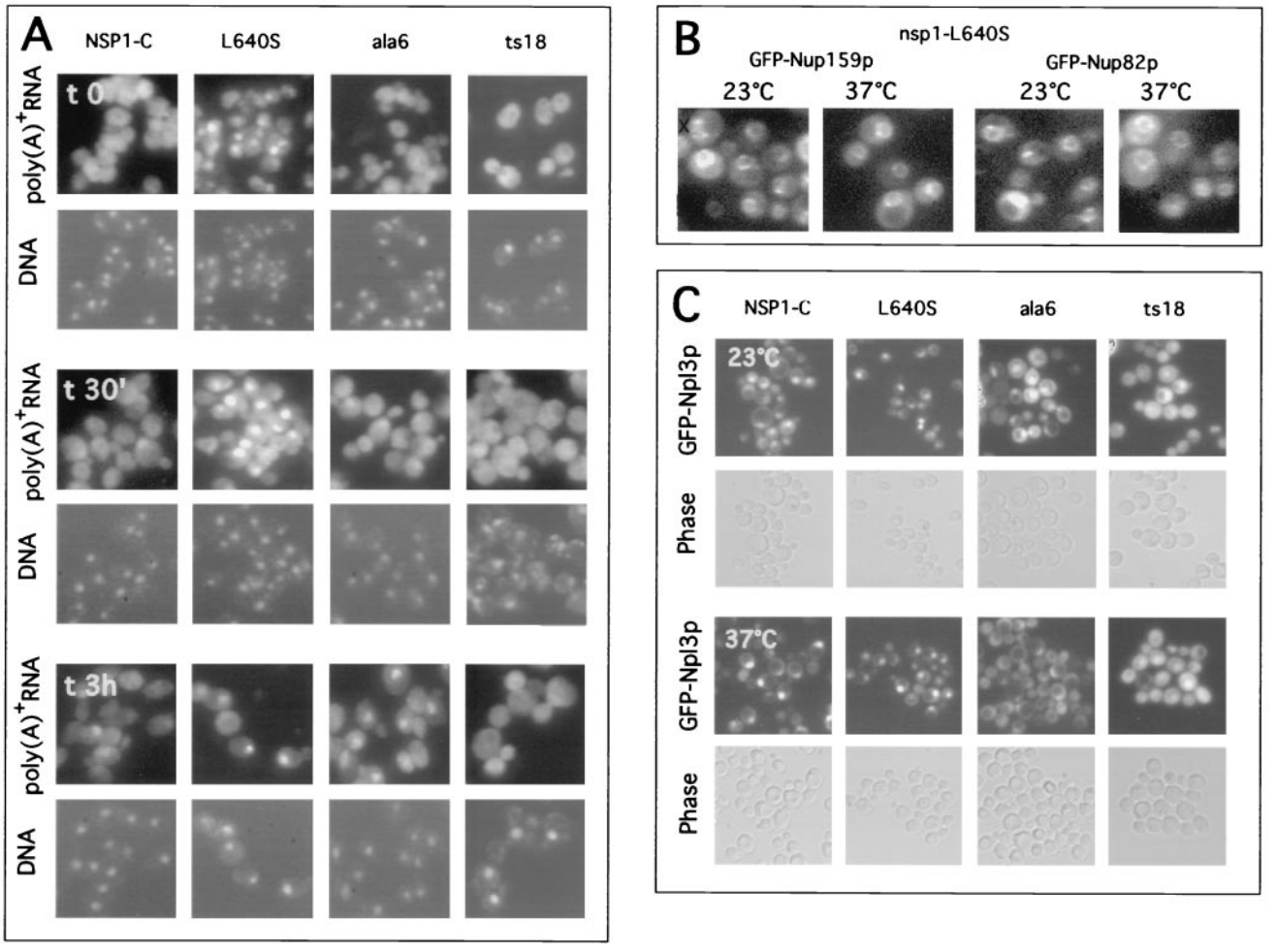

FIG. 4. Roles of the various coiled-coil regions of Nsp1p-C in nucleocytoplasmic transport. (A) Nuclear poly(A)$^+$ RNA export. *NSP1-C* or *nsp1-L640S*, *nsp1-ala6*, and *nsp1 ts18* cells were grown at 23°C before a shift to 37°C for 0 min, 30 min, or 3 h. The localization of poly(A)$^+$ RNA was analyzed by in situ hybridization with a Cy3-labeled oligo(dT) probe. DNA was visualized by 4′,6′-diamidino-2-phenylindole (DAPI) staining. (B) NPC localization of GFP-Nup82p or GFP-Nup159p in *nsp1-L640S* cells as revealed by fluorescence microscopy. Cells were grown in selective media at 23°C or shifted to 37°C for 2 h. (C) Nuclear protein import. *NSP1-C*, *nsp1-L640S*, *nsp1-ala6*, and *nsp1 ts18* cells expressing GFP-Npl3p were grown in selective media at 23°C or shifted to 37°C for 3 h and analyzed by fluorescence microscopy. In each case, the *nsp1*Δ strain was complemented by a plasmid expressing the corresponding mutant (see Table 2).

4 are not required for Nsp1p complex formation but are important for its in vivo function raised the question of their specific role in NPC structure and function. Therefore, we tested whether the different Nsp1p coiled-coil regions have distinct functions in nucleocytoplasmic transport. Nuclear protein import was analyzed in the various *nsp1* ts mutants by using the nuclear reporter GFP-Npl3p (Fig. 4C) (39). Evidently, nuclear import of GFP-Npl3p is strongly impaired in the *nsp1 ts18* (coil 3 and 4) and *nsp1-ala6* (coil 2) mutants (Fig. 4C; see also reference 3). In contrast, nuclear accumulation of GFP-Npl3p is not inhibited in the *nsp1-L640S* coil 1 mutant. However, when nuclear poly(A)$^+$ RNA export was analyzed in the *nsp1-L640S* mutant, severe inhibition was already seen at the permissive temperature, which increased further after a shift for 30 min to 37°C (Fig. 4A). In contrast, the *nsp1-ala6* mutant exhibited only a mild export defect and the *nsp1 ts18* mutant exhibited no mRNA export defect (Fig. 4A). It is known that a C-terminal *nup82* or *nup159* mutation affects the stability of the Nup82p complex and its association with the NPC, followed by inhibition of poly(A)$^+$ RNA export (3, 8, 19). Thus, mutations in Nsp1p coil 1 could affect the targeting of the Nup82p complex to the NPCs, thereby impairing nuclear mRNA export. However, GFP-tagged Nup82p and Nup159p are still localized at the nuclear pores in the coil 1 mutant *nsp1-L640S* (Fig. 4B).

Taken together, these data show a role of Nsp1p coil 2 in both nuclear import and export reactions, most likely because this region organizes two different heterodimeric subcomplexes with roles in nuclear protein import and mRNA export, respectively. In addition, adjacent coiled-coil regions 1, 3, and 4, although not required for complex assembly, are linked to specific nucleocytoplasmic transport processes (see Discussion).

Nsp1p coils 3 and 4 mediate efficient docking of the Nsp1p-Nup57p-Nup49p complex at the NPC. To find out why *nsp1* coil 3 and 4 mutants are predominantly impaired in nuclear protein import, Nsp1p mutated in coiled-coil region 3 and

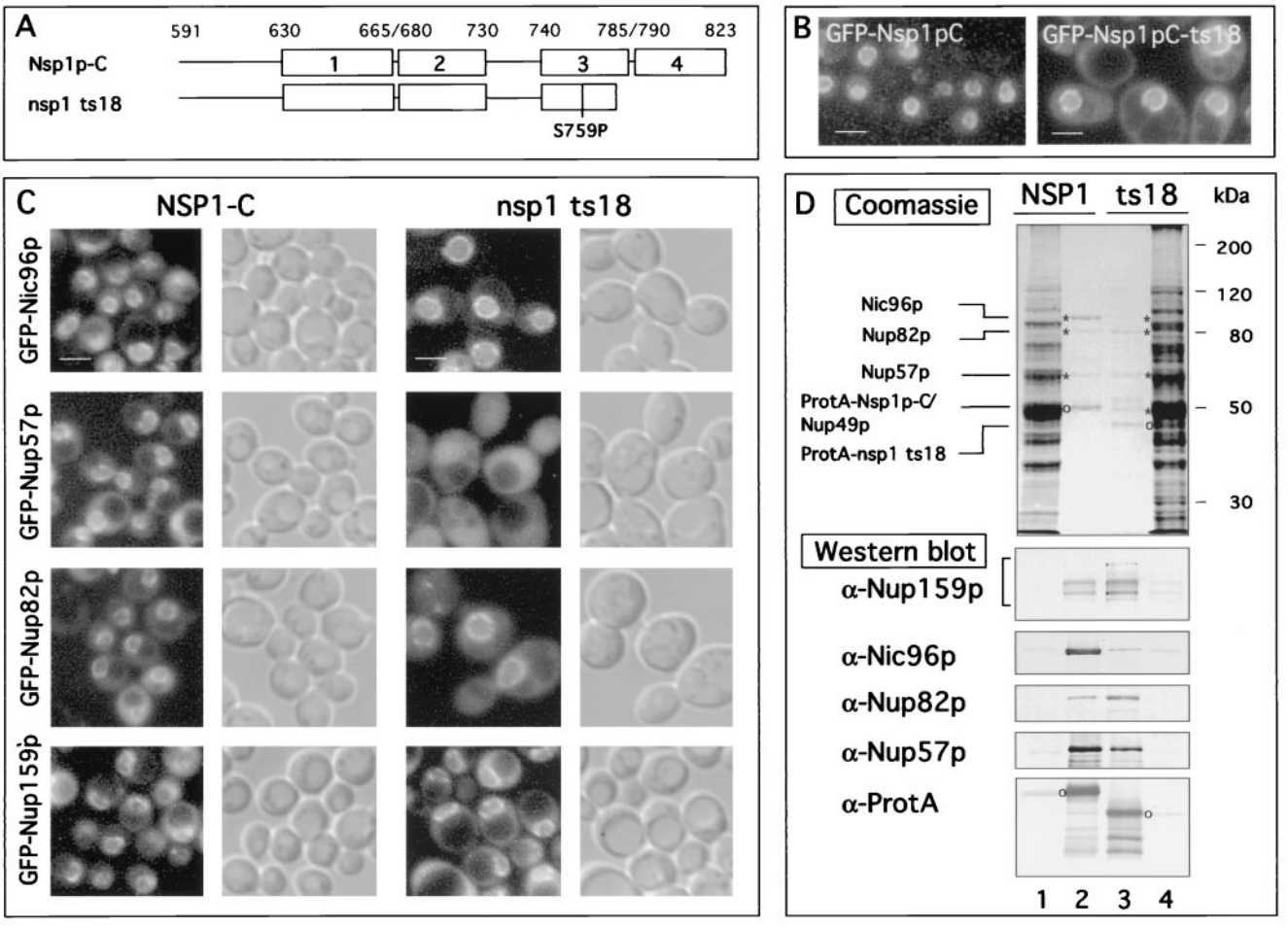

FIG. 5. Nsp1p coils 3 and 4 are required for docking of the Nsp1p-Nup57p-Nup49p complex to the NPC. (A) Schematic drawing of *nsp1 ts18*. (B) Localization of GFP-*NSP1-C* and GFP-*nsp1 ts18* expressed in *nsp1*Δ cells. Bars, 4 μm. (C) Localization of GFP-Nic96p, GFP-Nup57p, GFP-Nup82p, and GFP-Nup159p in *nsp1*Δ/*nupX*Δ strains (see Table 1) complemented by two plasmids expressing *NSP1-C* or *nsp1 ts18* cells and GFP-NupXp. Cells were grown in selective media at 23°C and analyzed by fluorescence microscopy or Nomarski optics. Bars, 4 μm. (D) Affinity purification of ProtA–Nsp1p-C and ProtA-*nsp1 ts18* expressed in *nsp1*Δ cells. Whole-cell lysates (lanes 1 and 4) or proteins eluted from IgG-Sepharose (lanes 2 and 3) were analyzed by SDS-PAGE and Coomassie staining or by Western blotting with anti-Nup159p, anti-Nic96p, anti-Nup82p, anti-Nup57p, and anti-ProtA antibodies. The positions of ProtA fusion proteins are indicated by open circles, and the positions of copurifying proteins are indicated by asterisks.

lacking coiled-coil region 4 (*nsp1 ts18*) was further characterized. GFP-tagged Nsp1p-S759P/Δ776–823 is still located at the nuclear envelope, but a considerable amount is detectable in the cytoplasm (Fig. 5B). In contrast, intact Nsp1p-C tagged with GFP is exclusively located at the nuclear envelope (Fig. 5B). Strikingly, GFP-Nup57p (Fig. 5C) and GFP-Nup49p (data not shown) are no longer targeted to the nuclear envelope in *nsp1 ts18* and are found predominantly in the cytoplasm. In contrast, GFP-Nic96p remains located at the NPCs (Fig. 5C). When GFP-Nup82p and GFP-Nup159p were tested, nuclear envelope labeling equal to or even stronger than that in *NSP1-C* cells was observed in *nsp1 ts18* cells (Fig. 5C).

To analyze the biochemical properties of both Nsp1p-C subcomplexes in the *nsp1 ts18* mutant, cells expressing ProtA–Nsp1p-C and ProtA-*nsp1 ts18* were grown at the permissive temperature. Following affinity purification by IgG-Sepharose chromatography, the purified ProtA fusion proteins were analyzed by SDS-PAGE and Coomassie staining or Western blotting. ProtA-*nsp1 ts18* and ProtA–Nsp1p-C, which are expressed in comparable amounts (data not shown), both coisolated Nup49p (data not shown) and Nup57p (Fig. 5D, lanes 2 and 3), indicating that the heterotrimeric Nsp1p-Nup49p-Nup57p complex still forms in the mutant. However, Nic96p, which is seen as a prominent 95-kDa band in the ProtA–Nsp1p-C eluate, is present in only small amounts in the ProtA-*nsp1 ts18* eluate (Fig. 5D). Thus, considering both the in vivo localization and the biochemical data, Nic96p remains associated with the NPCs in *nsp1 ts18* mutant cells, whereas the core Nsp1p-Nup57p-Nup49p complex forms but is not assembled into the NPCs. In contrast to Nic96p, Nup82p and Nup159p copurify very well with ProtA-*nsp1 ts18* (Fig. 5D, lane 3). Thus, consistent with the in vitro binding of Nup82p to Nsp1p coil 2, a region unaffected by the *nsp1 ts18* mutation, the NPC association and the biochemical stability of the Nup82p complex are unaltered in *nsp1 ts18* mutant cells.

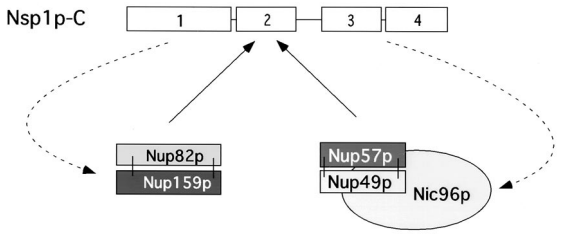

FIG. 6. Model of interaction of Nup82p-Nup159p and Nup57p-Nup49p-Nic96p, respectively, with Nsp1p-C.

DISCUSSION

Nsp1p, one of the most abundant Nups, has a central role in organizing two distinct NPC subcomplexes, Nsp1p-Nup49p-Nup57p-Nic96p and Nsp1p-Nup82p-Nup159p, which perform different roles in nucleocytoplasmic transport (3, 18–20, 32). To find out how the essential Nsp1p-C can mediate these different functions, a novel in vitro reconstitution assay was established that allows affinity purification of Nsp1p subcomplexes from urea-denatured recombinant Nups. In principle, this method should be applicable to investigation of the interaction of other recombinant proteins that are insoluble in *E. coli*.

Based on coiled-coil predictions, the essential Nsp1p-C consists of four subdomains, Nsp1p coils 1 to 4 (37). An intriguing question was whether the same or a different Nsp1p-C subdomain organizes the Nsp1p-Nup49p-Nup57p-Nic96p and Nsp1p-Nup82p-Nup159p complexes. We identified a relatively short region within Nsp1p-C (residues 673 to 738) that is the platform to accommodate both heterodimeric complexes. In particular, Nup57p and Nup82p bind to coiled-coil region 2 of Nsp1p-C but not to the flanking regions. Most importantly, binding of Nup57p and that of Nup82p to Nsp1p-C are mutually exclusive and Nup57p and Nup82p compete for the same binding site on Nsp1p-C. Thus, both heterotrimeric complexes are formed at the same central region within Nsp1p-C. How the correct stoichiometric ratio between the two subcomplexes is generated in vivo remains to be shown. Furthermore, it is not clear whether Nsp1p-C can dynamically be exchanged from one NPC subcomplex to the other or whether the complexes, once formed, are kinetically stable (see also below).

The components of the Nsp1p-Nup57p-Nup49p-Nic96p complex are located on both sides of the central gated channel (12). We show here that a coil 3 and 4 mutation of Nsp1-C (e.g., *nsp1 ts18*) allows assembly of a core Nsp1p-Nup57p-Nup49p complex, while targeting of this core complex to the pores is impaired. Thus, docking of the Nsp1p-Nup57p-Nup49p complex to the NPC depends not only on its integrity and on the amino-terminally located coiled-coil domain of Nic96p (this study; 4) but also on the presence of Nsp1p coils 3 and 4 (4, 20). Thus, in the model that emerges from these studies, Nsp1p coil 2 binds to Nup57p while Nup57p attracts Nup49p; this formed core complex requires adjacent coiled-coil regions, such as coils 3 and 4, for docking to Nic96p, thereby triggering a stable association with the NPC (Fig. 6).

Our in vitro reconstitution assay has further revealed that Nup82p directly interacts with Nsp1p coil 2 and that the presence of Nup82p enhances the binding of Nup159p-C to Nsp1p-C. Previous data showed that Nup159p and Nsp1p-C form a complex independent of Nup82p and that Nup82p interacts with Nup159p in blot overlay experiments (3, 26). It will be interesting to find out which of the Nsp1p coiled-coil regions binds to Nup159p, but this is difficult to test in our in vitro assay, since Nup159p-C nonspecifically binds to GSH-beads. Taken together, the data suggest that each of the three proteins in the Nup82p complex can interact with both neighbors in order to form a stable Nup82p complex. Interestingly, mutations within Nsp1p coil 3 and Nsp1p coil 4 do not interfere with docking of GFP-Nup82p and GFP-Nup159p at the NPC or with the integrity of the Nup82p complex. Thus, consistent with previous results, the NPC association of the Nup82p complex is unaffected by the absence or dissociation of the Nsp1p-Nup57p-Nup49p complex (4).

Mutations in *NUP82* or *NUP159* lead to specific defects in poly(A)$^+$ RNA export (1, 8, 16, 19, 25, 26). Therefore, it was intriguing that some of the *nsp1-C* mutants tested were not significantly defective in poly(A)$^+$ RNA export, although they showed inhibition of nuclear protein import. This could mean that the import defect is manifested earlier than the export defect. Alternatively, allele-specific *nsp1* mutants may exist that are defective in either nuclear protein import or nuclear mRNA export. During these studies, we looked more systematically into this issue and identified the *nsp1-L640S* ts allele as strongly defective in nuclear mRNA export but not in nuclear import of GFP-Npl3p. This suggests that coiled-coil region 1 within Nsp1p-C is specifically linked to the mRNA export machinery. Since this domain is not required for complex formation with Nup82p and Nup159p, it may have a supplementary function in vivo. One possibility is that further components of the mRNA export machinery interact with coiled-coil domain 1 of Nsp1p-C. Interestingly, the *nsp1-L640S* allele was previously used for synthetic lethal screens and led predominantly to components involved in poly(A)$^+$ RNA export (e.g., *NUP116*, *NUP145*, *NUP85*, and *NUP84*) (44). In addition, the *nsp1-L640S* mutation is synthetically lethal with *nup116* Δ*GLEBS* and with a *gle2* null allele (1; Bailer and Hurt, unpublished data). Thus, *nsp1-L640S* is strongly linked to nuclear mRNA export. It is therefore possible that Nsp1p coil 1 is crucial in association with Nup82p, Nup159p, and the Nup116p-Gle2p complex.

How formation of yeast NPC subcomplexes is regulated, how they are assembled into NPCs, and what determines their stoichiometric ratios are largely unexplored. In this context, it is worth mentioning that the Nsp1p-Nup49p-Nup57p-Nic96p and Nsp1p-Nup82-Nup159p complexes not only differ in function and localization within the NPC. Preliminary data indicate that the Nup82p complex is less abundant than the Nup57p complex (Bailer and Hurt, unpublished data; see also reference 35). We found that both the Nup57p and Nup82p complexes are formed in the same region within Nsp1p-C. This could indicate that biogenesis of both Nsp1p-C complexes in vivo is a competitive process that needs to be coordinated and regulated. Our experiments showed that similar amounts of Nup57p were coisolated with *ProtA-nsp1 ts18* or ProtA–Nsp1p-C, whereas the amount of Nup82p was strongly increased when *ProtA-nsp1 ts18* was affinity purified. We cannot exclude the possibility that this was caused by a difference in stability between the *ProtA-nsp1 ts18* subcomplexes. Despite that, it is intriguing to speculate that dissociation of the

Nup57p complex from the NPC favors the formation of the Nup82p complex. Indeed, the fluorescence intensity of GFP-Nup82p and GFP-Nup159p seems increased in *nsp1 ts18* and *nup57-E17* mutants, both of which affect the integrity and NPC interaction of the Nup57p complex (4; this study).

Attempts to overexpress Nup82p to compete in vivo for NPC binding of GFP-Nup57p and vice versa were unsuccessful. Similarly, overexpression of an isolated Nsp1p coil 2 region had no effect on the localization of GFP-Nup57p or GFP-Nup82p. Finally, NPC localization of GFP-Nup82p or GFP-Nup57p in the *nsp1-ala6* mutant after shifting of the cells to the restrictive temperature was unaltered (Bailer and Hurt, unpublished data). These negative data can easily be explained by multiple interactions of both Nsp1p subcomplexes with neighboring proteins that cannot be competed by overexpression of just one component. Alternatively, overexpression of only one Nup without stoichiometric expression of the corresponding binding partner(s) could cause self-aggregation, as observed by Carmo-Fonseca et al. (6). Apart from these difficulties in showing in vivo competition between Nup82p and Nup57p for binding to the Nsp1p coil 2 region, our in vitro data clearly demonstrate this competitive situation.

In summary, we have molecularly dissected the Nic96p-Nsp1p-Nup57p-Nup49p and Nup82p-Nup159p-Nsp1p complexes and investigated the modular organization of Nsp1p-C. A central region of Nsp1p-C is sufficient for in vitro formation of both Nsp1p subcomplexes, while flanking regions harbor functions involved in nuclear protein import and mRNA export processes. Future analysis will reveal the regulation of their assembly and integration into the NPC. Thus, the coiled-coil domain of Nsp1p is more structured than initially anticipated.

ACKNOWLEDGMENTS

We thank C. Cole (Dartmouth Medical School, Hanover, N.H.) for kindly providing us with polyclonal antibodies against Nup159p and the Nup159p shuffle strain. J. Aris (University of Florida) provided us with antibodies against Nsp1p. We greatly appreciate the generous help of several members of the Hurt laboratory, particularly that of Thomas Gerstberger and Karina Deinert.

E.C.H. is the recipient of a grant from the Deutsche Forschungsgemeinschaft (SFB352) and an HFSP grant.

REFERENCES

1. **Bailer, S. M., C. Balduf, J. Katahira, A. Podtelejnikov, C. Rollenhagen, M. Mann, N. Pante, and E. Hurt.** 2000. Nup116p associates with the Nup82p-Nsp1p-Nup159p nucleoporin complex. J. Biol. Chem. **275:**23540–23548.
2. **Bastos, R., L. Ribas de Pouplana, M. Enarson, K. Bodoor, and B. Burke.** 1997. Nup84, a novel nucleoporin that is associated with CAN/Nup214 on the cytoplasmic face of the nuclear pore complex. J. Cell Biol. **137:**989–1000.
3. **Belgareh, N., C. Snay-Hodge, F. Pasteau, S. Dagher, C. N. Cole, and V. Doye.** 1998. Functional characterization of a Nup159p-containing nuclear pore subcomplex. Mol. Biol. Cell **9:**3475–3492.
4. **Bucci, M., and S. R. Wente.** 1998. A novel fluorescence-based genetic strategy identifies mutants of Saccharomyces cerevisiae defective for nuclear pore complex assembly. Mol. Biol. Cell **9:**2439–2461.
5. **Buss, F., and M. Stewart.** 1995. Macromolecular interactions in the nucleoporin p62 complex of rat nuclear pores: binding of nucleoporin p54 to the rod domain of p62. J. Cell Biol. **128:**251–261.
6. **Carmo-Fonseca, M., H. Kern, and E. C. Hurt.** 1991. Human nucleoporin p62 and the essential yeast nuclear pore protein NSP1 show sequence homology and a similar domain organization. Eur. J. Cell Biol. **55:**17–30.
7. **Dabauvalle, M. C., K. Loos, and U. Scheer.** 1990. Identification of a soluble precursor complex essential for nuclear pore assembly in vitro. Chromosoma **100:**56–66.
8. **Del Priore, V., C. Heath, C. Snay, A. MacMillan, L. Gorsch, S. Dagher, and C. Cole.** 1997. A structure/function analysis of Rat7p/Nup159p, an essential nucleoporin of Saccharomyces cerevisiae. J. Cell Sci. **110:**2987–2999.
9. **Doye, V., and E. C. Hurt.** 1995. Genetic approaches to nuclear pore structure and function. Trends Genet. **11:**235–241.
10. **Doye, V., R. Wepf, and E. C. Hurt.** 1994. A novel nuclear pore protein Nup133p with distinct roles in poly(A)$^+$ RNA transport and nuclear pore distribution. EMBO J. **13:**6062–6075.
11. **Fahrenkrog, B., J. P. Aris, E. C. Hurt, N. Pante, and U. Aebi.** 2000. Comparative spatial localization of protein-A-tagged and authentic yeast nuclear pore complex proteins by immunogold electron microscopy. J. Struct. Biol. **129:**295–305.
12. **Fahrenkrog, B., E. C. Hurt, U. Aebi, and N. Pante.** 1998. Molecular architecture of the yeast nuclear pore complex: localization of Nsp1p subcomplexes. J. Cell Biol. **143:**577–588.
13. **Finlay, D. R., E. Meier, P. Bradley, J. Horecka, and D. J. Forbes.** 1991. A complex of nuclear pore proteins required for pore function. J. Cell Biol. **114:**169–183.
14. **Fornerod, M., J. van Deursen, S. van Baal, A. Reynolds, D. Davis, K. G. Murti, J. Fransen, and G. Grosveld.** 1997. The human homologue of yeast CRM1 is in a dynamic subcomplex with CAN/Nup214 and a novel nuclear pore component Nup88. EMBO J. **16:**807–816.
15. **Gorlich, D., and U. Kutay.** 1999. Transport between the cell nucleus and the cytoplasm. Annu. Rev. Cell Dev. Biol. **15:**607–660.
16. **Gorsch, L. C., T. C. Dockendorff, and C. N. Cole.** 1995. A conditional allele of the novel repeat-containing yeast nucleoporin RAT7/NUP159 causes both rapid cessation of mRNA export and reversible clustering of nuclear pore complexes. J. Cell Biol. **129:**939–955.
17. **Grandi, P., T. Dang, N. Pante, A. Shevchenko, M. Mann, D. Forbes, and E. Hurt.** 1997. Nup93, a vertebrate homologue of yeast Nic96p, forms a complex with a novel 205-kDa protein and is required for correct nuclear pore assembly. Mol. Biol. Cell **8:**2017–2038.
18. **Grandi, P., V. Doye, and E. C. Hurt.** 1993. Purification of NSP1 reveals complex formation with 'GLFG' nucleoporins and a novel nuclear pore protein NIC96. EMBO J. **12:**3061–3071.
19. **Grandi, P., S. Emig, C. Weise, F. Hucho, T. Pohl, and E. C. Hurt.** 1995. A novel nuclear pore protein Nup82p which specifically binds to a fraction of Nsp1p. J. Cell Biol. **130:**1263–1273.
20. **Grandi, P., N. Schlaich, H. Tekotte, and E. C. Hurt.** 1995. Functional interaction of Nic96p with a core nucleoporin complex consisting of Nsp1p, Nup49p and a novel protein Nup57p. EMBO J. **14:**76–87.
21. **Guan, T., S. Muller, G. Klier, N. Pante, J. M. Blevitt, M. Haner, B. Paschal, U. Aebi, and L. Gerace.** 1995. Structural analysis of the p62 complex, an assembly of O-linked glycoproteins that localizes near the central gated channel of the nuclear pore complex. Mol. Biol. Cell **6:**1591–1603.
22. **Ho, A. K., T. X. Shen, K. J. Ryan, E. Kiseleva, M. A. Levy, T. D. Allen, and S. R. Wente.** 2000. Assembly and preferential localization of Nup116p on the cytoplasmic face of the nuclear pore complex by interaction with Nup82p. Mol. Cell Biol. **20:**5736–5748.
23. **Hu, T., T. Guan, and L. Gerace.** 1996. Molecular and functional characterization of the p62 complex, an assembly of nuclear pore complex glycoproteins. J. Cell Biol. **134:**589–601.
24. **Hurt, E., S. Hannus, B. Schmelzl, D. Lau, D. Tollervey, and G. Simos.** 1999. A novel in vivo assay reveals inhibition of ribosomal nuclear export in ran-cycle and nucleoporin mutants. J. Cell Biol. **144:**389–401.
25. **Hurwitz, M. E., and G. Blobel.** 1995. NUP82 is an essential yeast nucleoporin required for poly(A)$^+$ RNA export. J. Cell Biol. **130:**1275–1281.
26. **Hurwitz, M. E., C. Strambio-de-Castillia, and G. Blobel.** 1998. Two yeast nuclear pore complex proteins involved in mRNA export form a cytoplasmically oriented subcomplex. Proc. Natl. Acad. Sci. USA **95:**11241–11245.
27. **Kita, K., S. Omata, and T. Horigome.** 1993. Purification and characterization of a nuclear pore glycoprotein complex containing p62. J. Biochem. (Tokyo) **113:**377–382.
28. **Kraemer, D. M., C. Strambio-de-Castillia, G. Blobel, and M. P. Rout.** 1995. The essential yeast nucleoporin NUP159 is located on the cytoplasmic side of the nuclear pore complex and serves in karyopherin-mediated binding of transport substrate. J. Biol. Chem. **270:**19017–19021.
29. **Macaulay, C., E. Meier, and D. J. Forbes.** 1995. Differential mitotic phosphorylation of proteins of the nuclear pore complex. J. Biol. Chem. **270:**254–262.
30. **Marelli, M., J. D. Aitchison, and R. W. Wozniak.** 1998. Specific binding of the karyopherin Kap121p to a subunit of the nuclear pore complex containing Nup53p, Nup59p, and Nup170p. J. Cell Biol. **143:**1813–1830.
31. **Nehrbass, U., E. Fabre, S. Dihlmann, W. Herth, and E. C. Hurt.** 1993. Analysis of nucleo-cytoplasmic transport in a thermosensitive mutant of nuclear pore protein NSP1. Eur J. Cell Biol. **62:**1–12.
32. **Nehrbass, U., H. Kern, A. Mutvei, H. Horstmann, B. Marshallsay, and E. C. Hurt.** 1990. NSP1: a yeast nuclear envelope protein localized at the nuclear pores exerts its essential function by its carboxy-terminal domain. Cell **61:**979–989.
33. **Nehrbass, U., M. P. Rout, S. Maguire, G. Blobel, and R. W. Wozniak.** 1996. The yeast nucleoporin Nup188p interacts genetically and physically with the core structures of the nuclear pore complex. J. Cell Biol. **133:**1153–1162.
34. **Ohno, M., M. Fornerod, and I. W. Mattaj.** 1998. Nucleocytoplasmic trans-

port: the last 200 nanometers. Cell **92:**327–336.
35. **Rout, M. P., J. D. Aitchison, A. Suprapto, K. Hjertaas, Y. Zhao, and B. T. Chait.** 2000. The yeast nuclear pore complex: composition, architecture, and transport mechanism. J. Cell Biol. **148:**635–651.
36. **Ryan, K. J., and S. R. Wente.** 2000. The nuclear pore complex: a protein machine bridging the nucleus and cytoplasm. Curr. Opin. Cell Biol. **12:**361–371.
37. **Schlaich, N. L., M. Haner, A. Lustig, U. Aebi, and E. C. Hurt.** 1997. In vitro reconstitution of a heterotrimeric nucleoporin complex consisting of recombinant Nsp1p, Nup49p, and Nup57p. Mol. Biol. Cell **8:**33–46.
38. **Schlenstedt, G., E. Hurt, V. Doye, and P. A. Silver.** 1993. Reconstitution of nuclear protein transport with semi-intact yeast cells. J. Cell Biol. **123:**785–798.
39. **Senger, B., G. Simos, F. R. Bischoff, A. Podtelejnikov, M. Mann, and E. Hurt.** 1998. Mtr10p functions as a nuclear import receptor for the mRNA-binding protein Npl3p. EMBO J. **17:**2196–2207.
40. **Sherman, Y., G. R. Fink, and J. B. N. Hicks (ed.).** 1986. A laboratory course manual. Cold Spring Harbor Laboratory Press, Cold Spring Harbor, N.Y.
41. **Siniossoglou, S., M. Lutzmann, H. Santo-Rosa, K. Leonhard, S. Mueller, U. Aebi, and E. Hurt.** 2000. Structure and assembly of the Nup84p complex. J. Cell Biol. **149:**41–53.
42. **Siniossoglou, S., C. Wimmer, M. Rieger, V. Doye, H. Tekotte, C. Weise, S. Emig, A. Segref, and E. C. Hurt.** 1996. A novel complex of nucleoporins, which includes Sec13p and a Sec13p homolog, is essential for normal nuclear pores. Cell **84:**265–275.
43. **Stoffler, D., B. Fahrenkrog, and U. Aebi.** 1999. The nuclear pore complex: from molecular architecture to functional dynamics. Curr. Opin. Cell Biol. **11:**391–401.
44. **Wimmer, C., V. Doye, P. Grandi, U. Nehrbass, and E. C. Hurt.** 1992. A new subclass of nucleoporins that functionally interact with nuclear pore protein NSP1. EMBO J. **11:**5051–5061.
45. **Zabel, U., V. Doye, H. Tekotte, R. Wepf, P. Grandi, and E. C. Hurt.** 1996. Nic96p is required for nuclear pore formation and functionally interacts with a novel nucleoporin, Nup188p. J. Cell Biol. **133:**1141–1152.
46. **Zentgraf, H., M. Frey, S. Schwinn, C. Tessmer, B. Willemann, Y. Samstag, and I. Velhagen.** 1995. Detection of histidine-tagged fusion proteins by using a high-specific mouse monoclonal anti-histidine tag antibody. Nucleic Acids Res. **23:**3347–3348.